Spatial dispersion in negative-index composite metamaterials

A. I. Căbuz,* D. Felbacq, and D. Cassagne
UMR 5650 CNRS, Université Montpellier II, Place E. Bataillon Bt 21, CC074, 34095 Montpellier Cedex 05, France
(Received 26 July 2007; published 11 January 2008)

The metamaterials exhibiting negative permittivity and permeability that have been under numerical and experimental study recently generally operate at frequencies between the homogeneous ($\lambda \gg$ period) and heterogeneous ($\lambda \approx$ period) regimes, a region characterized by the phenomenon of spatial dispersion. However, since many interesting applications such as the superlens rely on nondispersive homogeneous behavior, one needs a means to diagnose spatial dispersion efficiently as well as to explore in more detail the physics of dispersive media. In this work, we put forward and illustrate the notion of an inhomogeneous effective medium model. We use it to explore the spatial dispersion in negative-index composites, and we show that it is an ideal tool for studying the behavior of composite metamaterials in the intermediate-frequency region where homogeneous effective medium models become spatially dispersive or nonlocal.

DOI: 10.1103/PhysRevA.77.013807 PACS number(s): 42.70.Qs, 77.84.Lf, 77.22.Ch, 78.20.Ci

I. INTRODUCTION

It is often said in the electromagnetic metamaterial literature that for wavelengths larger than the period one can treat the material as a homogeneous medium. However, an aspect that is given far less attention is that of how large the wavelength needs to be, of how one knows when the wavelength is sufficiently large for a homogeneous model to be useful, and of what happens when the wavelength is not sufficiently large. These questions are the starting point of this work.

Whenever one considers a medium that operates in the intermediate region between the homogeneous ($\lambda \gg$ period) and the inhomogeneous ($\lambda \approx$ period) regimes, one has a choice of two different points of view. First, one may try to deal with the composite medium in its full three-dimensional glory, taking explicitly into account the detailed spatial distribution of the medium properties, e.g., dielectric constant and conductivity. This requires heavy use of numerical simulations in order to take into account all the detail of the material structure. Alternatively, one may use a homogeneous model, where the position-dependent properties of the medium are replaced with an effective homogeneous model, with the caveat that the effective homogeneous parameters (at a given frequency and field polarization) may exhibit a dependence on the wave vector **k**.

However, most novel applications of composite metamaterials (superlens, invisibility cloak) require effective parameters independent of the wave vector. Moreover, spatially dispersive homogeneous parameters cannot be seen properly as properties of the medium, but rather as descriptions of the interaction between the medium and the field. As physicists studying the properties of the materials we are thus inclined to consider a spatially dispersive description as incomplete, in some sense. This point of view is detailed considerably in Sec. III below.

The paper is organized as follows. Section II introduces the two main sources of spatial dispersion in metamaterials: the wire-resonator coupling, and the size of the wavelength in relation to the period. The former has already been treated theoretically in the literature and this work focuses mainly on the latter. Our approach is conceptually outlined in the fundamental discussion of Sec. III where the concept of the *inhomogeneous effective medium model* is introduced and discussed in detail. The ideas and intuitions developed in Sec. III are used in the rest of the work, and are tested and supported by the numerical results of Sec. VI.

II. SPATIAL DISPERSION

In the context of this work we use the term "spatial dispersion" to refer to the phenomenon whereby the permittivity and/or permeability tensors describing a given medium exhibit a dependence on the wave vector **k** of the field. Media exhibiting this behavior are also often termed "nonlocal" due to the fact that the polarization field at a given point depends on the electric or magnetic field over a *finite volume* surrounding that point. Nonlocal behavior and spatial dispersion are two terms for the same physical phenomenon, viewed in direct space or reciprocal space, respectively. In the following the terms "nonlocal" and "spatially dispersive" will be used interchangeably, with a preference for the former in Sec. III. Photonic crystals are a prime example of this kind of complex behavior. Due to the development of accurate numerical methods for the analysis of these structures [1], their spatially dispersive properties can be controlled to the extent that they have generated a plethora of new applications. However, while in the case of photonic crystals spatial dispersion is a "feature," and it can be put to good use, in the case of negative-index metamaterials it is a "bug," and for the most interesting applications, such as the superlens [2] or the cloak [3–5], it must be avoided.

Several different metamaterial designs have been put forward for the realization of a negative-index of refraction [6–10]. However, none have been studied in as much depth and detail, either theoretically or experimentally, as the wire-resonator composite put forward by Pendry and co-workers [11,12]. Consequently, it is on this design that our study focuses, with the sole modification of using the nonbianisotro-

*alexcabuz@gmail.com

pic broadside coupled resonator design of Marques *et al.* [13].

Two main sources of spatial dispersion in negative-index composites can be identified. The first is related to the magnetic interaction of wires and resonators, while the second is related to the size of the wavelength compared to the structure period. We discuss each in turn.

It has been pointed out [14,15] that thin-wire media exhibit strong spatial dispersion even in the quasistatic limit for incident waves where the electric field is not exactly parallel to the wires (otherwise known as conical incidence). In the quasistatic limit it is still possible to define an effective permittivity, though it depends on the direction of propagation:

$$\varepsilon_z(k,k_z) = \varepsilon_0\left(1 - \frac{k_0^2}{k^2 - k_z^2}\right). \tag{1}$$

Here k_0 is the free-space wave vector, and k is the wave vector in the medium in which the wires are embedded. k_z is the component of the wave vector that is parallel to the wires. Since a component of the wave vector appears explicitly in the formula for the permittivity, this is a prime example of a spatially dispersive permittivity. In the special case of $k_z=0$, that is, incidence in the plane normal to the wires, the spatial dispersion disappears due to the translational symmetry of the structure. This translational symmetry, however, strictly holds only in a medium composed of wires only. In a composite structure where resonators are present in the spaces between the wires, the translational symmetry is broken, and, as Simovski *et al.* [16] point out, spatial dispersion becomes a distinct possibility once again, even in the plane normal to the wires. This issue of the near-field coupling between wires and resonators has been discussed by several authors [17–19], and it was shown by Maslovski [20] that this undesirable effect can be avoided by a careful placement of wires and resonators such as to decouple their magnetic interactions. This is a result which is crucial for the development below, in particular in Sec. VI.

The second possible cause of spatial dispersion in negative-index composites is an operating wavelength too small compared to the structure period. It has become common practice in the study of negative-index composites to use experimental or numerical data obtained from transmission studies in normal incidence in order to support claims of a negative index of refraction. The parameter extraction method [21] has become particularly popular for these purposes. However, this method is almost always used only for normal-incidence studies, and there are few studies considering off-normal incidence [22–24], which is the only way to truly test for spatially dispersive features.

In this work we study composite metamaterials as a function of both frequency and angle of incidence, and we show that, by placing resonators at nodes of the magnetic field of the wires, spatial dispersion can be avoided. Moreover, we put forward an intermediate-homogenization model whereby the composite is approximated by a stack of homogeneous slabs, where each slab has either a negative permittivity or a negative permeability. Since this stack is intermediate between the three-dimensional (3D) composite and the homogeneous effective medium, it may be used to gauge how "far" the two are from each other, as explained below. The conceptual basis of the notion of an inhomogeneous effective medium is laid out in Sec. III (and in more detail in Chap. 1 of Ref. [25]) and confirmed by the numerical results of Sec. VI.

The construction of the homogeneous as well as the inhomogeneous effective medium model discussed in Sec. III requires a thorough understanding of wire media and resonator media. This is addressed in Secs. IV and V, where we discuss analytical models of split-ring resonators and wires, respectively. In Sec. VI we put them together and show that the wavelength-to-period ratios commonly employed in the literature are too small to avoid spatial dispersion (as also suggested in Ref. [24]). We show how this shortcoming can be avoided by modifying the magnetic resonators to shift the resonance to longer wavelengths, thus eliminating spatial dispersion in a certain frequency range.

III. INHOMOGENEOUS EFFECTIVE MEDIA

Homogenization is the process whereby the complicated and cumbersome microscopic fields existing in a heterogeneous medium are replaced by smoothly varying (or macroscopic) fields which, though ignoring the details on the scale of the heterogeneity, are still useful for characterizing the behavior of the medium. In essence, at a given wavelength, the field propagation in a given medium is independent of the microscopic details of the structure, being sensitive only to its macroscopic, average properties. Homogenization can therefore be seen as the process whereby all the (presumably useless) microscopic information is discarded, leaving only the useful, macroscopic information.

As we will see below, an important caveat to this process is that the blurring of the microscopic details of the field and the charge distribution implicitly makes the description nonlocal. In other words, once in the macroscopic world, the notion of a "point" must be blurred into the notion of a "ball." One can no longer properly speak of any point in space to within less than a certain distance that is related to the amount of blurring that has been done, or to the amount of microscopic information that has been discarded in the homogenization process. We therefore expect macroscopic fields to be related to each other in a nonlocal way related to how blurred the microscopic picture is by the homogenization process. We come back to these ideas below.

In order for homogenization to be useful, one must have a way of discriminating between microscopic and macroscopic scales. Periodic media are a perfect case for studying these issues, due to the simplification brought about by Bloch's theorem. It tells us that the reciprocal space representation of a field propagating in a periodic lattice contains contributions from a discrete set of spatial frequencies. In a one-dimensional structure with period d, these correspond to $k_B + nK$ where $K=2\pi/d$, n is an integer, and k_B is the Bloch wave vector of the propagating wave.

The essential step in the homogenization process is the spatial averaging. This is done using an averaging volume $f(\mathbf{x})$ discussed by Russakoff [26]. Spatial averaging then

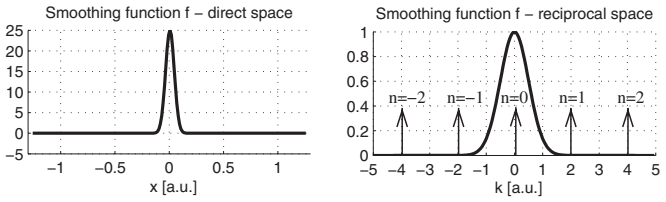

FIG. 1. Smoothing function $f(\mathbf{x})$ in one dimension—case of very large wavelength.

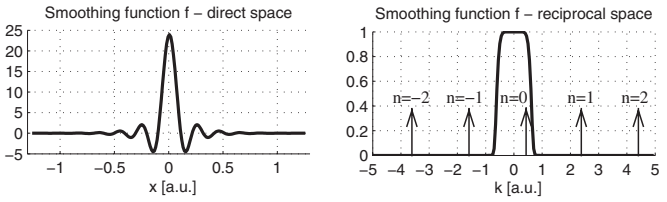

FIG. 2. Smoothing function $f(\mathbf{x})$ in one dimension—case of shorter wavelength.

takes the mathematical form of a convolution integral. The macroscopic field $\mathbf{E}(\mathbf{x})$ corresponding to the microscopic quantity $\mathbf{e}(\mathbf{x})$ is then defined as

$$\mathbf{E}(\mathbf{x}) \equiv \int d^3x' f(\mathbf{x}')\mathbf{e}(\mathbf{x}-\mathbf{x}') \equiv f(\mathbf{x}) \circ \mathbf{e}(\mathbf{x}), \tag{2}$$

where the small circle denotes convolution. It is the size of this averaging volume, $f(\mathbf{x})$, that tells us how much blurring is being done. This is the size of the ball inside which the *macroscopic* description cannot see, making it a nonlocal description.

This definition is illustrated graphically in Fig. 1 for the case of very large wavelength. In direct space (left plot), the convolution integral implies that the macroscopic field at the origin depends on the microscopic field over a certain region about the origin. In this case the averaging volume is around 0.2 a.u. across. In reciprocal space (right plot), the convolution becomes a product and the averaging volume becomes simply a low-pass filter on the spatial frequencies composing the "signal," which in this case is the microscopic electric field $\mathbf{e}(\mathbf{x})$. Homogenization requires that only the lowest spatial harmonic be kept, and that all the higher harmonics be averaged over, or filtered out.

Let us consider the impact of the spatial averaging on the definition of the susceptibility: $\mathbf{P}(\mathbf{k})=\chi(\mathbf{k})\mathbf{E}(\mathbf{k})$. In direct space this takes the form of a convolution integral:

$$\mathbf{P}(\mathbf{x}) = \chi(\mathbf{x}) \circ \mathbf{E}(\mathbf{x}) = \int d^3x' \chi(\mathbf{x}-\mathbf{x}')\mathbf{E}(\mathbf{x}'). \tag{3}$$

Since, as argued above, the macroscopic description has been blurred by the spatial averaging, we expect the susceptibility to have a size similar to the averaging volume. In other words, the macroscopic polarization at some point in space is expected to depend on the macroscopic field over a region of similar size to the averaging volume $f(\mathbf{x})$. But let us consider what happens in the case of very large wavelength. In that case the macroscopic electric field can be considered constant over a region as large as the averaging volume, and the electric field can be taken out of the above integral. The macroscopic polarization becomes

$$\mathbf{P}(\mathbf{x}) \approxeq \mathbf{E}(\mathbf{x}) \int d^3x' \chi(\mathbf{x}-\mathbf{x}') = \chi_{\mathrm{dc}}\mathbf{E}(\mathbf{x}), \tag{4}$$

where χ_{dc} is the dc component of the susceptibility. In this case, for all intents and purposes, the susceptibility acts as if it were singular, $\chi_{\mathrm{eff}} \approxeq \chi_{\mathrm{dc}}\delta(\mathbf{x})$, and the macroscopic model acts as if it were local. In essence, the implicit nonlocality of the macroscopic description is hidden by the size of the wavelength. The electric field acts as a low-pass filter, in a sense, on the observed susceptibility, and the blurring due to the spatial averaging is not detectable.

This works well as long as the wavelength of the macroscopic field in the medium is much larger than the averaging volume, so that the field can be considered constant over the extent of the averaging volume. In this case the macroscopic model acts as if it is local, and therefore exhibits no spatial dispersion. This is the situation most widely considered in textbooks or other contexts.

However, as the wavelength becomes shorter, the nonlocality must inevitably come into its rights. Indeed, as soon as the electric field is no longer approximately constant over volumes of the size of $f(\mathbf{x})$ the finite size of the susceptibility starts to make itself felt, with the result that one must once again write $\mathbf{P}(\mathbf{x})=\chi(\mathbf{x})\circ\mathbf{E}(\mathbf{x})$. This process is accelerated by the fact that, as illustrated in Fig. 2, as the wavelength decreases, the Bloch wave vector moves away from the origin in reciprocal space, requiring a change in the filter function $f(\mathbf{k})$ (right plot), which results in a larger averaging volume in direct space (left plot). Thus as the wavelength decreases the averaging volume must increase, with the result that there comes a point where the variation of the field over the averaging volume can no longer be ignored.

Such a nonlocal description of the medium can still be useful, but it is clear that a local description is more general, because it does not require knowledge of the wave vector (e.g., direction of propagation) of the incident field. In this sense a local description is more complete, because it contains enough information about the medium that a detailed knowledge of the field (other than its frequency) is not necessary. It would therefore be desirable to have a way of obtaining a local model of the medium. And the way to do this is simple in principle: we must choose a smaller averaging function, one sufficiently small that the electric field may be considered as constant over it, making it possible to apply the above argument whereby the nonlocality is hidden.

But reducing the size of the averaging volume has one other important consequence: it renders the description inhomogeneous. This can be seen on Fig. 2. As $f(\mathbf{x})$ becomes smaller in direct space, $f(\mathbf{k})$ must become larger in reciprocal space, with the result that the higher harmonics, with $n=\pm 1$, are no longer filtered out. The effective medium model is now no longer homogeneous, since it contains harmonics periodic on the scale of the microscopic unit cell. By adjusting $f(\mathbf{x})$ we have traded in nonlocality in exchange for inhomogeneity.

In this context, effective medium theory can be seen as a box, with one adjustment knob on it, $f(\mathbf{x})$. When it is large,

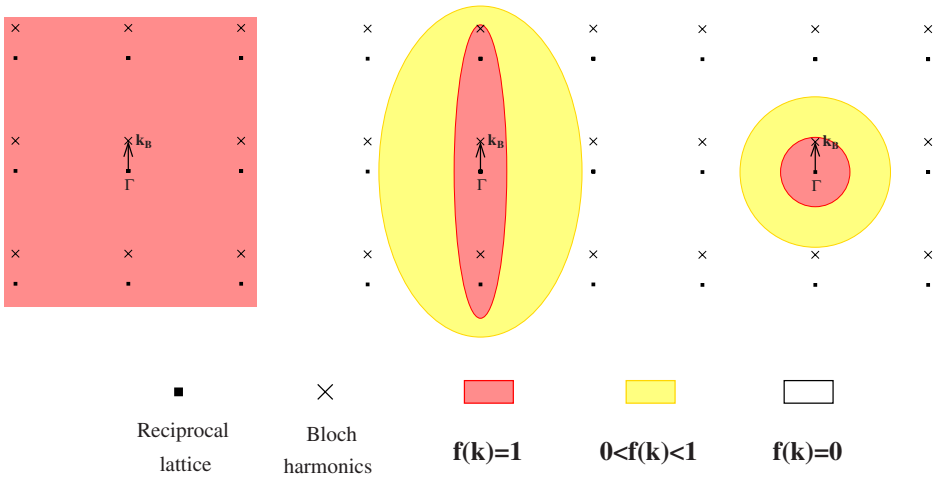

FIG. 3. (Color online) Three possible models corresponding to three $f(\mathbf{k})$ functions. The first is the one where all harmonics are kept, corresponding in real space to $f(\mathbf{x})=\delta(\mathbf{x})$ the Dirac delta function. The model on the right is a homogeneous model; only the lowest harmonic is kept, the rest are filtered out. The case in the middle is an intermediate model, where two of the y harmonics are kept. All three models are effective medium models, but only the one on the right is homogeneous. But is it also local?

the model is homogeneous, though possibly nonlocal. When it is smaller, the nonlocality may be avoided, at the cost of the model becoming inhomogeneous. This knob provides us with a prescription for obtaining custom-made effective medium models. In some cases we may prefer the local description, and in some cases we may prefer the homogeneous description. Even though this tradeoff is irrelevant at very large wavelengths (in that case we may have both, as shown above), it becomes inevitable at wavelengths approaching the periodicity of the structure.

It is useful to visualize these ideas also in two dimensions. This is done in Fig. 3. We have plotted schematically the filter function $f(\mathbf{k})$ in reciprocal space. The dots represent the reciprocal lattice of the medium, while the crosses indicate the positions of the Bloch harmonics of the field propagating in the lattice. The filter's pass regions are represented in red (darker shading), stop regions are represented in white, while yellow (lighter shading) is intermediate (the function must be continuous and as smooth as possible [25,26]). The case on the left corresponds to the identity filter, in this context, the Dirac δ in direct space. The pass region of the filter extends indiscriminately to the whole reciprocal space, and the effective medium model can be seen as the identity model. The case on the right corresponds to a homogeneous effective medium model, which filters out all harmonics other than the lowest, the one in the first Brillouin zone. The case in the middle is an intermediate case: in addition to the lowest harmonic the filter lets pass also the first y harmonics. The result is an inhomogeneous model, a 1D structure periodic in the vertical direction.

Now let us imagine that we do not know whether the homogeneous model is local or not. In other words, and as stated above, we do not know whether it contains enough information about the medium that knowledge of the field distribution is unnecessary. Now, if it did not, that would mean that some of the harmonics which have been filtered out actually contain important information about the behavior of the medium. This leads to a picture whereby information about the medium is seen as clustered at points in reciprocal space corresponding to the Bloch components of the quasiperiodic field propagating in the structure (the crosses in Fig. 3). This view in turn leads naturally to the following two testable predictions.

(1) If the homogeneous model and the 1D model disagree (give different transmission and reflection coefficients for normal incidence, for instance) at a given frequency, then the homogeneous model is nonlocal, and it also disagrees with the identity model. We expect this because, if the 1D intermediate model disagrees with the homogeneous model, this implies that the y harmonics which are included in the 1D model contain important information about the medium, and cannot be ignored, meaning that the homogeneous model is incomplete and therefore nonlocal.

(2) If the homogeneous model agrees with the identity model, then it is local, and it also agrees with the 1D intermediate model. We expect this because, if the homogeneous and the identity model agree, then this implies that the information contained in all the higher harmonics is irrelevant so that the homogeneous model is complete and therefore local.

Before going any further we should respond to an objection that might immediately be brought against, for instance, the second prediction. One may imagine that all the higher Bloch harmonics might combine in such a way in the identity model as to give the same result as the homogeneous model, but without also agreeing with the 1D model. The higher harmonics might be irrelevant together but not separately. However, this cannot happen in any consistent fashion due to the fact that all the Bloch harmonics are mutually orthogonal. Thus, if by some extremely unlikely coincidence, at a given frequency and angle of incidence, both the magnitude and phase of the transmission coincide for the identity and the homogeneous models, this could be immediately identified as an accidental occurrence by varying the parameters slightly (frequency or angle of incidence). If the agreement melts away, then one can be confident it is simply an accident of no physical significance.

In Sec. VI we test the above predictions numerically. However, it should be pointed out that, even though the arguments of this section can be used as a computational prescription for the numerical analysis of metamaterials, the authors of this work have preferred to take a more analytical approach to the analysis of the particular geometry studied here. The reason why is simply "because we can." In more complicated structures the analytical approach used here is impractical, and a more brute force computational method of direct 3D spatial averaging as described above is required.

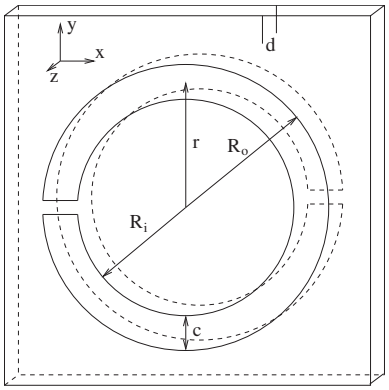

FIG. 4. Broadside coupled resonator.

However, the fact that in the context of this work the ideas of this section are used rather as guides for the intuition than as actual computational prescriptions does not in the least diminish their computational significance. Several suggestions for further research in this direction are made below, in the Conclusion.

IV. MAGNETIC RESONATORS

Several approaches to the analytical modeling of metallic magnetic resonators have been attempted. Among these we may note, in order of increasing complexity (and accuracy), the work of Sauviac *et al.* [27], that of Marques *et al.* [13,28], and that of Shamonin *et al.* [29]. Sauviac *et al.* proceed by approximating the metal strips as circular wires, and using existing analytic formulas (see Ref. [30]). Marques *et al.* take explicitly into account the strip geometry with its edge effects through the formulas of Ref. [31]. Shamonin *et al.* go even further by accounting for the nonuniform distribution of current and charge density over the circumference of the metal rings. While the first two approaches can hope to obtain only the fundamental resonance, that of Shamonin *et al.* is accurate even for higher resonances.

All three approaches mentioned above rely on an equivalent circuit picture of the resonator. Each ring is seen as an effective *RLC* circuit (lumped for the first two approaches or distributed for Shamonin *et al.*'s approach), and they are coupled by the mutual inductance and the mutual capacitance. Our discussion assumes no loss mechanism, setting R to zero, with a more detailed discussion provided below. Our goal is therefore to obtain estimates of the two essential quantities, the effective inductance and the effective capacitance characterizing the magnetic resonance.

The resonator design we study here is the nonbianisotropic broadside coupled resonator proposed by Marques *et al.* [13] (see Fig. 4). Each resonator consists of two rings of thin perfectly conducting metal strips of width c, inner radius R_i, and outer radius R_o where $R_o - R_i = c$. The mean radius is $r = (R_o + R_i)/2$. The two rings are separated by distance d. The magnetic resonance is excited by magnetic fields along the axis of the resonator (z axis in this case). There is also an electric response due to the polarization of the metal rings. This electric response is sensitive to the orientation of the electric field with respect to the ring splits. The behavior and therefore the analysis is simpler if the electric field is directed along the x axis, since in this case the splits play no role. Consequently, in the composite metamaterial the wires will also be oriented in the same direction. The geometry of the material is represented schematically in Fig. 5.

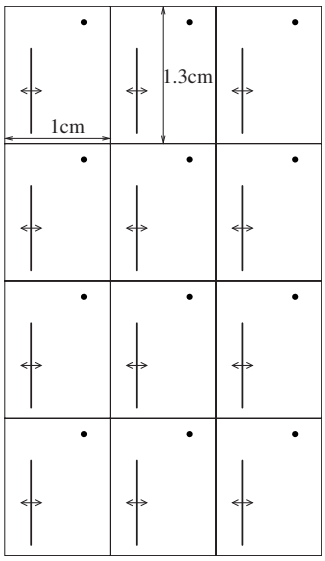

FIG. 5. Schematic metamaterial geometry. The finite-element simulation is done on a sample four periods thick in the vertical direction and periodic in the horizontal direction. The electric field is directed out of the page, along the wires, while the magnetic field is in the plane of the page. Arrows indicate orientation of magnetic moments of resonators.

Following the analysis of Ref. [27], the magnetic polarizability of the resonators takes the frequency-dependent form

$$\gamma^m = \frac{2\omega^2 \mu_0 S^2}{L(\omega^2 - \omega_i^2)} \tag{5}$$

where $S = \pi r^2$ and $\omega_i = 1/\sqrt{LC}$. The resonators are placed in a lattice with a rectangular unit cell of volume $V = 1 \times 1 \times 1.3\ \mathrm{cm}^3 = 1.3\ \mathrm{cm}^3$. The Mossotti-Clausius relation then tells us that the effective permeability of the resonator medium is given by

$$\mu_z = 1 + \frac{\gamma^m}{V - \gamma^m/3}. \tag{6}$$

We now come to the issue of estimating the crucial parameters L and C. In the course of our investigations we began by using the simplest available model, that of Ref. [27]. The agreement with the full-vector 3D finite-element numerical results was remarkably good, but only for geometries with d much smaller than c, corresponding to fairly low resonance frequencies (see, in particular, Figs. 6 and 7, where the analytical model of Sauviac *et al.* is compared with the numerical results). For larger distances between metal strips the analytical model lost its accuracy, and we henceforth obtained all parameters by fitting the numerical results. For the interested reader the details of the analytical development are available in Sec. 3.6 of Ref. [25], while Table I contains the

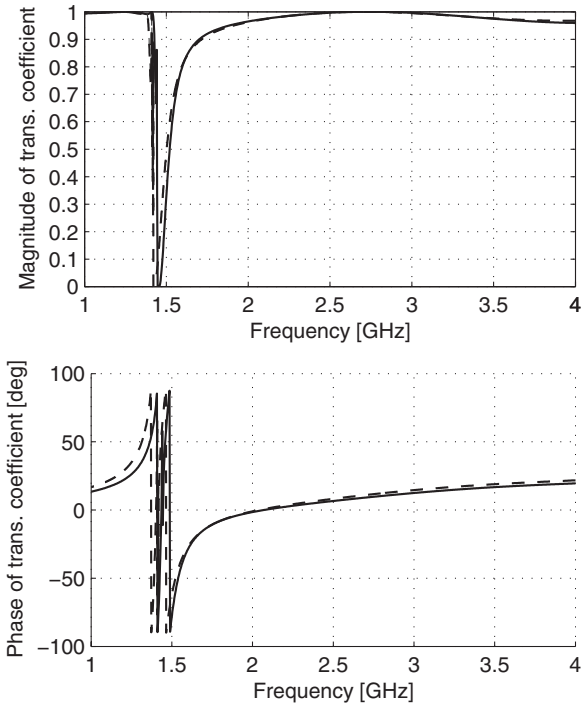

FIG. 6. Magnitude (top) and phase (bottom) of the transmission coefficient for normal incidence onto a slab of four layers of resonators with R_o=4 mm, R_i=3 mm, and d=0.05 mm. 3D finite-element calculation (solid) and analytical effective medium theory (dashed).

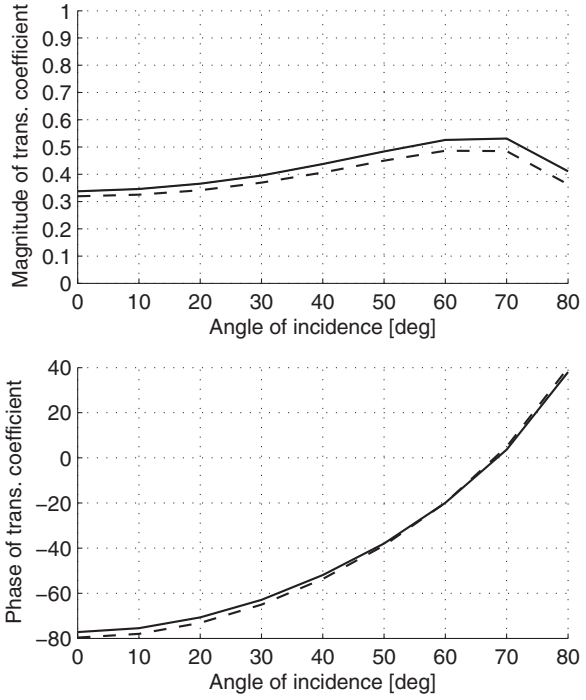

FIG. 7. Magnitude (top) and phase (bottom) of the transmission coefficient for a slab of four layers of resonators with R_o=4 mm, R_i=3 mm, and d=0.05 mm at a frequency of f=1.5 GHz (λ=20 cm) and for an incidence angle varying between 0° and 80°. At this frequency we have effective permeabilities μ_x=−0.838, μ_y=1, and μ_z=1. The effective permittivity is ε_y=1.41. 3D finite-element calculation (solid) and effective medium theory (dashed).

values obtained by fitting Eqs. (5) and (6) to the numerical results. The reason the analytical model works better when the distance between metal strips, d, is small is that the capacitance used does not account for edge effects, which are weak when $d \ll c$.

We now come back to the issue of the loss term represented by the resistive element in our *RLC* model of the resonators. At first it might seem that, since the metal elements are perfectly conducting, there is no loss mechanism, but in fact radiative losses must always be present in order to satisfy energy conservation. If a resonator is to be able to receive energy from an incident wave, it must also be able to radiate energy back into space. Otherwise the field intensity and the energy locked inside the resonator would increase without limit with time. This aspect is discussed in detail by Yatsenko *et al.* [32,33]. The polarizability of the scattering particle (in our case the resonator) must have an imaginary component due to radiative loss, given by

$$\mathrm{Im}\left(\frac{1}{\gamma^m_{\mathrm{cplx}}}\right) = \frac{k^3}{6\pi\mu_0}. \tag{7}$$

Of course, this results in a complex-valued magnetic polarizability, even for dissipationless particles, γ^m_{cplx}. However, this is not the same polarizability that is introduced in the Mossotti-Clausius relation. This is due to the fact that, once the particles are placed in an infinite 3D periodic lattice, the energy balance must take into account not only the incident wave and scattered wave power for a single particle, but also the waves scattered by all the other particles. In essence, the derivation of the Mossotti-Clausius relation already takes into account the radiative interaction between a given scatterer and the rest of the lattice through the notion of the local field seen by the scatterer. This is why the polarizability that must be used in the Mossotti-Clausius relation is an effective real polarizability given by [33]

$$\gamma^m = \frac{1}{\mathrm{Re}(1/\gamma^m_{\mathrm{cplx}})}. \tag{8}$$

We should also point out that in practice, and for the configurations we have considered, this correction, though required for physical rigor, is small outside a very small frequency range close to the magnetic resonance. Moreover,

TABLE I. Effective capacitance and inductance of broadside coupled split-ring resonators for different geometries.

R_o (cm)	R_i (cm)	d (cm)	L^{eff} (nH)	C^{eff} (pF)
0.4	0.3	0.005	21.39	0.534
0.4	0.3	0.01	20.63	0.298
0.37	0.3	0.02	15.76	0.203
0.37	0.3	0.04	16.79	0.11
0.37	0.3	0.06	16.32	0.09
0.37	0.3	0.08	14.64	0.087
0.37	0.3	0.1	13.52	0.086

this small frequency range is best avoided in any case since the effective parameters of the medium are divergent there and the effective medium model breaks down.

We now come to the electric response of the resonators. This response is due to the fact that an applied electric field along the x axis results in a polarization of the metal particle. An analytical formula for the polarizability of a pair of loops of radius r of perfectly conducting cylindrical wire of radius r_w is given by [34]

$$\gamma^e = \frac{4\pi^2 r^3}{\ln(8r/r_w) - 2}. \tag{9}$$

However, since the polarization properties of the resonator are expected to depend to some extent on the shape of the metal strips, and since this formula is obtained by replacing the strips by round wires, it is only a fairly coarse approximation. Fortunately, it turns out that the electric response of the resonators is very weakly dependent on both the frequency and the distance between the loops. Thus we seek a single number, and the value that is consistent with all the simulations below is $\varepsilon_x = 1.41$. We use it for the rest of this work.

By arranging the resonators of Fig. 4 one per unit cell we expect to obtain, in the large-wavelength limit, an anisotropic medium, with a possibly negative permeability in the z direction and a permittivity of 1.41 in the x direction. The permeability in the other directions is expected to be that of free space since the resonators have no magnetic response in directions other than the z direction.

In order to test the analytical model described above we compare its predictions with results of 3D finite-element simulations obtained using the commercial numerical computation package CST MICROWAVE STUDIO. The solid curves are the 3D finite-element simulations, while the dashed curves correspond to the effective medium model. Figures 6 and 7 compare the magnitude and phase of the transmission coefficient as a function of frequency for normal incidence and as a function of angle of incidence at a frequency of 1.5 GHz. The agreement is excellent for this type of resonator.

It should, however, be pointed out that, while the agreement between theory and simulation is very good in this case, this is no longer the case when the metal strips are brought further apart. The edge effects modify the capacitance. Consequently, in general, a certain amount of parameter fitting is required in order to make the analytical model fit the 3D numerical results. Values of the effective capacitance and effective inductance deduced from numerical simulations are given in Table I for various resonator geometries.

V. THIN-WIRE MEDIUM

In this section we outline our model for the infinite 2D thin-wire medium in the case of a rectangular unit cell. The approach we take is to model each row of wires as an infinitely thin impedance plane characterized by a monodromy matrix $\mathbf{T}_W$. The monodromy matrix formalism is presented in Refs. [35,36]. Within this formalism a row of thin metal wires of period $d=2\pi/K$ and radius r_w can be represented by the very simple matrix [37]

$$\mathbf{T}_W = \begin{pmatrix} 1 & 0 \\ \frac{2}{L} & 1 \end{pmatrix}, \tag{10}$$

where $L=-(2/K)\ln(Kr_w)$, while a slab of homogeneous dielectric of thickness a and permittivity ε is represented by the matrix

$$\mathbf{T}(a,\varepsilon) = \begin{pmatrix} \cos\left(\frac{\beta a}{2}\right) & \frac{1}{\beta}\sin\left(\frac{\beta a}{2}\right) \\ -\beta\sin\left(\frac{\beta a}{2}\right) & \cos\left(\frac{\beta a}{2}\right) \end{pmatrix}, \tag{11}$$

where $\beta^2 = k^2\varepsilon - k^2\sin^2\phi$. The matrix associated with a period of the 2D wire medium is obtained by sandwiching a row of wires between two slabs of homogeneous dielectric. If each row has a period d and they are stacked with period h in a medium of permittivity ε_m, then the matrix describing a period is given by

$$\mathbf{M} = \mathbf{T}(h/2,\varepsilon_m)\times\mathbf{T}_W\times\mathbf{T}(h/2,\varepsilon_m) = \begin{pmatrix} \cos(\beta h) + \frac{1}{\beta L}\sin(\beta h) & \frac{2}{\beta^2 L}\sin^2\left(\frac{\beta h}{2}\right) + \frac{1}{\beta}\sin(\beta h) \\ -\beta\sin(\beta h) + \frac{2}{L}\cos^2\left(\frac{\beta h}{2}\right) & \cos(\beta h) + \frac{1}{\beta L}\sin(\beta h) \end{pmatrix}. \tag{12}$$

By comparing this matrix with the matrix of a homogeneous slab of the same thickness h and unknown effective permittivity ε_{eff}, $\mathbf{T}(h,\varepsilon_{\text{eff}})$ (see Fig. 8), one can extract an expression for the effective permittivity:

$$\varepsilon_{\text{eff}} = \varepsilon_m + \frac{1}{k^2h^2}\left[\arccos\left(1+\frac{h}{L}\right)\right]^2. \tag{13}$$

The validity of this model is confirmed by the results of Fig. 9. The solid curves are obtained using the 3D frequency domain finite-element solver of CST MICROWAVE STUDIO software package, while the dashed curves are obtained using the transfer matrix method described in Ref. [38] applied to a homogeneous dielectric slab with permittivity ε_{eff} given by Eq. (13). The thin curves correspond to wires in free space ($\varepsilon_m=1$) while the thick curves correspond to wires inter-

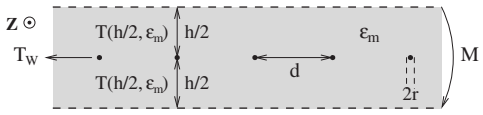

FIG. 8. We obtain a homogeneous model for the wire grating by adding layers of the surrounding medium on the top and the bottom of the grating. The total monodromy matrix given by $\mathbf{M}=\mathbf{T}(h/2,\varepsilon_m)\times\mathbf{T}_W\times\mathbf{T}(h/2,\varepsilon_m)$ is compared with the monodromy matrix of a homogeneous layer of the same total thickness h, $\mathbf{T}(h,\varepsilon_{\text{eff}})$.

spersed with closed resonators ($\varepsilon_m=1.41$). These results, along with those of Figs. 6 and 7, are consistent with an effective permittivity of 1.41 for the resonator medium.

VI. COMPOSITE MEDIUM: THE 1D STACK MODEL

In Sec. II above, we have mentioned the two main sources of spatial dispersion in composite metamaterials. We now show how to avoid them such that the medium be spatial-dispersion-free. We begin with the near-field coupling between wires and resonators.

The issue of the wire-resonator coupling has been discussed by several authors, beginning with the work of Pokrovsky and Efros [17], who showed that when very thin infinite wires are placed in a medium with a negative permeability the resulting structure does not exhibit a negative permittivity and that therefore a negative-index medium cannot be obtained in this way. The authors then proceeded to conclude that thin metallic wires cannot be used to provide the negative permittivity required to obtain a negative-index medium. This disconcerting conclusion was, however, later shown to be premature in a comment by Marqués and Smith [18] and the more detailed analyses of Felbacq *et al.* [19,39,40], but the fact remains that the near-field coupling between wires and resonators is detrimental to the negative-permittivity property of the composite.

Thus it seems that a strong interaction between wires and resonators is undesirable for two different reasons: the appearance of spatial dispersion, as discussed in Sec. II, and the

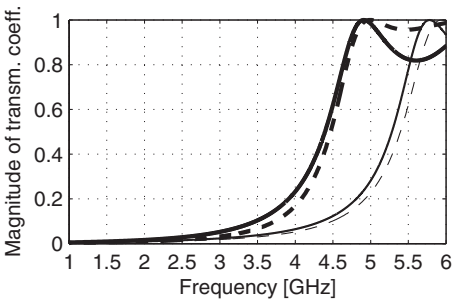

FIG. 9. Magnitude of the transmission coefficient of wires alone (thin curves) and of wires and closed resonators (thick curves) as a function of frequency. Dashed curves are given by Eq. (13) with $\varepsilon_m=1$ (red) and 1.41 (green). The wires are of radius 0.05 mm and the structure is composed of four rows of period 1 cm and spaced by 1.3 cm from each other.

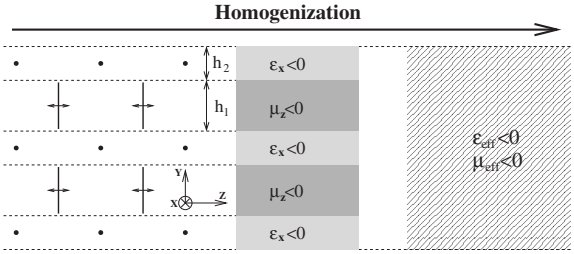

FIG. 10. Homogenization as a progression corresponding to the smoothing functions depicted schematically in Fig. 3.

disappearance of the negative permittivity [16]. Perhaps the most straightforward clarification of this issue is due to Maslovski [20], who argued that the solution is to place the resonators at the nodes of the magnetic field of the wires, as illustrated in Fig. 5. In this way the wires and resonators are magnetically decoupled due to the symmetry, and the wires behave independently of the magnetic activity of the resonators. The capacitive coupling remains, but this can be reduced by simply placing wires and resonators farther apart, or equivalently using smaller resonators. The results below will show that, by placing the resonators as suggested by Maslovski, spatial dispersion can be avoided, and the homogenization of composite metamaterials is possible.

But the interaction of resonators and wires is not the only possible source of spatial dispersion in composite metamaterials. In fact, as is well known, the most common source of spatial dispersion is the proximity of the scales of the wavelength and the period of the structure in which the wave is propagating, $\lambda\approx d$. The question becomes "How large should the wavelength be if the structure is to behave as a *local* homogeneous medium?" In order to get a handle on this issue, we make use of the ideas of Sec. III.

The main idea is illustrated in Fig. 10. The homogenization of negative-index composites is usually done by replacing the 3D structure with a homogeneous medium with effective parameters ε_{eff} and μ_{eff} which are obtained either constructively (as above) or holistically (as with the parameter extraction procedure). In our approach we break up the homogenization process into two steps by introducing an intermediate model. It is obtained by homogenizing the structure to obtain an inhomogeneous effective medium, a 1D slab stack which mimics the structure of the composite. We are basically smoothing over all spatial harmonics in the periodic 3D structure except for the lowest harmonic and also the first y harmonics. All traces of periodicity are wiped out except for the y periodicity. The 1D stack mimics the geometry of the composite in the sense that each row of wires is replaced by a negative-permittivity slab, and each plane of resonators is replaced by a negative-permeability slab.

Our first task is to specify the effective medium parameters of the homogeneous model, ε_{eff} and μ_{eff}. This is greatly facilitated in our case due to the crucial result of Maslovski [41], which tells us that if correctly placed the electromagnetic activity of wires and resonators can be practically decoupled. There are only two possible ways in which they may interact: first through the dielectric activity of the resonators, and second through the capacitive coupling between the wires and the resonators, which modifies the effective

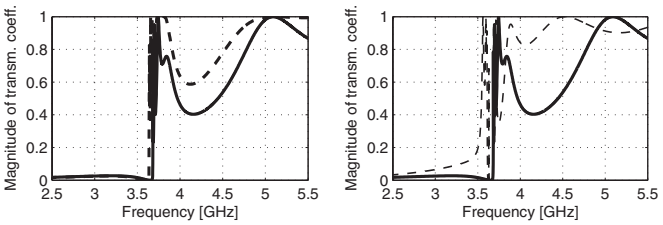

FIG. 11. Magnitude of the transmission coefficient as a function of frequency; resonators with $R_o=3.7$ mm, $R_i=3$ mm, and $d=0.4$ mm. 3D composite (solid), homogeneous model (dashed thick—left), and single negative stack (dashed thin—right).

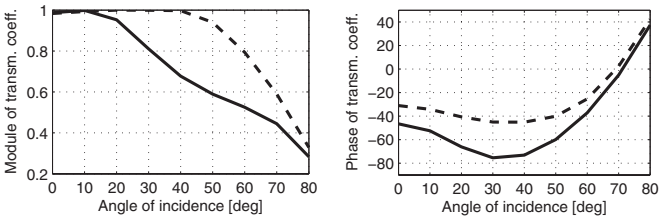

FIG. 12. Magnitude and phase of transmission coefficient as a function of angle of incidence. 3D composite (solid) and effective medium (dashed). The frequency is $f=3.748$ GHz. The effective medium values at this frequency are $\mu_{\text{eff}}=-1.13$ and $\varepsilon_{\text{eff}}=-0.412$.

internal capacitance of the resonators and thereby slightly shifts their resonance. The first is accounted for through the ε_m of Eq. (13), while the second influence is weak (less than 10%, as shown below) and can be included phenomenologically. The latter interaction can also be reduced through an optimized design, particularly by reducing the size of the resonators or by increasing the distances between resonators and wires.

We now obtain the parameters of the 1D single negative stack. The overall homogeneous medium parameters are given by the equations of previous sections. The unit cell is 13 mm deep, and the resonators are 8 mm across. Consequently, we model the structure as a slab stack with $h_1=8$ mm and $h_2=5$ mm with $\mu_2=1$ and where μ_1, ε_1, and ε_2 are fixed by requiring

$$\frac{h_1+h_2\varepsilon_2}{h_1+h_2}=\varepsilon_{\text{eff}}^{\text{wires alone}},$$

$$\frac{h_1\mu_1+h_2}{h_1+h_2}=\mu_{\text{eff}}^{\text{res. alone}},$$

$$\frac{h_1\varepsilon_1+h_2}{h_1+h_2}=\varepsilon_{\text{eff}}^{\text{res. alone}}, \tag{14}$$

where $\varepsilon_{\text{eff}}^{\text{wires alone}}$ is given by Eq. (13) and $\mu_{\text{eff}}^{\text{res. alone}}$ by Eqs. (5) and (6), and $\varepsilon_{\text{eff}}^{\text{res. alone}}=1.41$. The permittivity and permeability are now position dependent, periodic with the period of the lattice, but in such a way that they average to the fully homogenized effective medium values ε_{eff} and μ_{eff}. In a sense, the homogenization of the composite metamaterial must "pass through" the homogenization of the single negative stack [42].

Our numerical tests begin with the second statement of our conjecture, which states that if the 1D stack is not homogenized, then neither is the 3D composite. The first structure we consider has the unit cell as on the left side of Fig. 10 with periods $p_x=p_z=1$ cm, $p_y=1.3$ cm, the wires have radius $r_w=0.05$ mm, and the resonators have $R_o=3.7$ mm, $R_i=3$ mm, and $d=0.4$ mm where d is the distance between the two metal loops composing each resonator. The results are shown in Fig. 11. The solid curves show the magnitude of the transmission coefficient through four periods of the composite, calculated using MICROWAVE STUDIO, the thick-dashed curve (left plot) corresponds to the effective medium model, and the thin-dashed curve (right plot) is obtained from the intermediate model, the single negative 1D stack. While all three models show interesting behavior around the magnetic resonance at 3.8 GHz, it is clear that they do not agree. In particular, the dashed curves do not agree with each other in the region of interest around 3.8 GHz.

According to our conjecture, therefore, we expect the composite to behave inhomogeneously in this region, which is just another way of saying that the spatial dispersion is expected to be strong. We test this expectation by simulating the composite structure as a function of angle of incidence and comparing it to the effective medium model. The results are shown in Fig. 12.

The plots show the magnitude and phase of the transmission coefficient through four periods of the metamaterial (solid) and the equivalent thickness of effective medium (dashed) at a frequency of 3.748 GHz for angles of incidence between 0 and 80°. It is clear that, even though the magnitudes of the transmission coefficients seem to be in agreement in normal incidence, this agreement is only accidental. Both the magnitude and the phase of the transmission coefficient disagree over a large range of oblique angles of incidence, and the effective medium model is not justified for this structure. The first of our two predictions stated at the end of the previous section has survived the test. We now proceed to test the second prediction.

A magnetic resonance at a wavelength about six times larger than the period of the structure is clearly not sufficient to justify a homogeneous model. The spatial dispersion is too strong. Consequently we change the design of our resonators to shift the resonance to lower frequencies. Specifically, by bringing the metal loops to within $d=0.1$ mm of each other, and broadening them to a width of $c=1$ mm ($R_o=4$ mm, $R_i=3$ mm), the resonance frequency is roughly halved, as can be seen on the left side of Fig. 13. According to our second prediction, in that frequency region where the composite metamaterial agrees with the effective medium model, we expect the two to agree also with the 1D stack model. This is confirmed in the case of the frequency region around 1.95 GHz as can be seen in Fig. 13.

We now check the spatially dispersive behavior of the composite by sweeping the angle of incidence for a frequency in the range where all three models seem to agree, that is between 1.94 and 1.98 GHz, roughly. Figure 14 shows the results for a frequency of 1.958 GHz. The agreement between the effective medium model (dashed) and the 3D composite (solid) is remarkable. Thus our conjecture has also survived the second test. It is by no means proved (a more

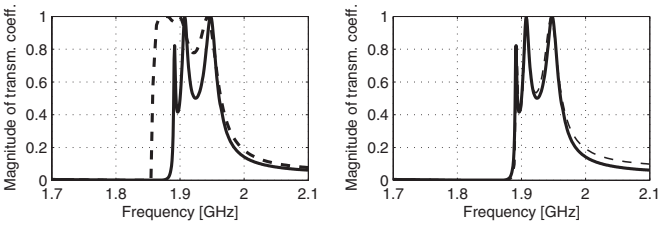

FIG. 13. Magnitude of the transmission coefficient as a function of frequency; resonators with $R_o=4$ mm, $R_i=3$ mm, and $d=0.1$ mm. 3D composite (solid), homogeneous model (dashed thick—left), and single negative stack (dashed thin—right).

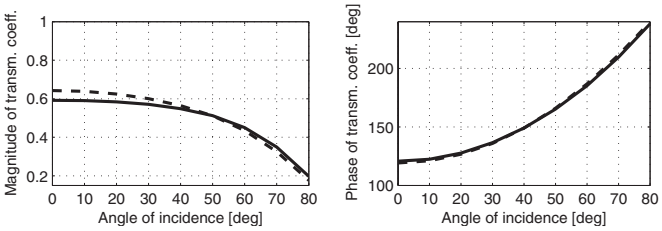

FIG. 14. Magnitude and phase of transmission coefficient as a function of angle of incidence. 3D composite (solid) and effective medium (dashed). The frequency is $f=1.958$ GHz and the wires are of radius 0.02 mm, a factor of 2.5 thinner than in Fig. 12. The effective medium values at this frequency are $\mu_{\text{eff}}=-0.295$ and $\varepsilon_{\text{eff}}=-4.332$.

mathematically rigorous approach would be required), but these results give us a fair amount of confidence as to its usefulness for purposes of testing tentative metamaterial designs before implementing them experimentally or even before undertaking tedious three-dimensional full vector simulations.

In the beginning of Sec. VI we argued that by placing the resonators at the nodes of the magnetic field of the wires the two types of elements would be inductively decoupled. However, they can still interact capacitively. In other words, the inductances in Table I are not modified when the resonators are integrated into the composite metamaterial, but the capacitances may be. Our simulations confirm this view. In fact Figs. 13 and 14 were obtained by using the same inductance as appears on the $d=0.01$ cm line of Table I though the capacitance had to be adjusted by about 10%. The effective capacitance that appears in the analytical model of the resonators is increased by about 30 pF by the presence of the wires. However, the fact that an agreement as good as that of Fig. 13 can be achieved by using the *same* inductance as for the resonators-alone structure confirms that our placement of the resonators truly decouples the resonators from the wires, at least for magnetic purposes. There remains only a weak capacitive coupling that can in principle be reduced by increasing the distances between the wires and the resonators, or, equivalently, making the resonators smaller.

VII. CONCLUSION

Composite metamaterials made of thin metal wires and magnetic resonators can exhibit spatial dispersion when the coupling between the resonators and wires is strong and/or when the wavelength is not sufficiently large compared to the period. In order to avoid this situation, it is necessary to place the metamaterial components so as to minimize their near-field interaction (inductive as well as capacitive) and to design the resonators to have a resonance wavelength that is sufficiently large compared to the period.

The optimal placement of the elements is obtained by placing the wires in a rectangular lattice, and the resonators also in a rectangular lattice, shifted from the first by half a unit vector in both directions. This ensures that the magnetic resonators are at nodes of the magnetic field of the wires, and that the symmetry of the structure decouples the two lattices as far as magnetic interactions are concerned. Our results provide numerical confirmation of the analytical arguments of Maslovski [20].

In order to determine whether the operating wavelength is sufficiently large compared to the period, one (time-consuming) way is to sweep the angle of incidence at fixed frequency and observe the spatial dispersion directly as reflected in the transmission or reflection coefficients. Another method is to use the 1D single-negative-stack model as a gauge. This intermediate model, which is described in detail above, allows a designer to quickly and efficiently locate frequency regions where a metamaterial is likely to behave as a homogeneous medium, or, if the metamaterial is not useful as a homogeneous effective medium, to diagnose it as such. This method can be applied in a straightforward way not only to Cartesian designs as was done here, but also to cylindrical geometries such as the electromagnetic cloak [3–5].

The ideas of Sec. III above, while illustrated here in a rather restricted context, have the potential to become a very powerful tool for analyzing and characterizing complex arbitrary metamaterials at wavelengths below the homogenization regime. They open up two research directions in particular.

The first is related to the fact that the structures that are most easily amenable to analytical treatment are often not also the most easily fabricated. In particular, a number of new structure types have been proposed recently [43,44], which experiments have shown to exhibit interesting behavior but for which an analytical approach seems difficult. In such structures it is not always clear what is the important region of the unit cell, for instance, from the point of view of the magnetic or the electric activity of the material. This question is important for reasons of design optimization. One would like to know, for instance, whether it is the thickness of the metal components, their length, their shape, or the distance separating them that dictates whether magnetic behavior will be observed at a given frequency. This question can be settled by using the above approach to create inhomogeneous models of these structures which will enable the designer to look *inside* the unit cell and gain a better understanding of the physical phenomena giving rise to the macroscopic behavior observed in the experiment (real or numerical), even if the wavelength is sufficiently large that the homogeneous behavior of the structure is not in question.

The second, and perhaps most interesting, possibility opened up by the ideas of Sec. III is the idea that composite metamaterials may be useful even for wavelengths that are

not large enough for the medium to behave as a homogeneous local medium. For wavelengths in the intermediate regime where spatial dispersion holds sway, the structure may be effectively modeled as an inhomogeneous effective medium, which may be seen as a metaphotonic crystal. This is an interesting concept, because it makes use of a frequency region hitherto considered useless, and, moreover, because this approach may allow the design of photonic crystals previously impossible to realize on the same scale. For instance, one may create novel periodic effective media, made up of interlocking negative-permittivity and negative-permeability regions, a possibility that goes far beyond current photonic crystal structures, which mainly consist of regions of naturally occurring dielectric alternating with regions of index equal to 1 (air holes). Classic numerical tools for the study of photonic crystals such as the MIT PHOTONIC BANDS software package may have to be updated to take into account the possibility of metaphotonic crystals, that is, effective photonic crystals made of combinations of truly arbitrary alternating media within the unit cell.

[1] S. G. Johnson and J. D. Joannopoulos, Opt. Express **8**, 173 (2001).
[2] J. B. Pendry, Phys. Rev. Lett. **85**, 3966 (2000).
[3] U. Leonhardt, Science **312**, 1777 (2006).
[4] J. B. Pendry, D. Schurig, and D. R. Smith, Science **312**, 1780 (2006).
[5] D. Schurig, J. J. Mock, B. J. Justice, S. A. Cummer, J. B. Pendry, A. F. Starr, and D. R. Smith, Science **314**, 977 (2006).
[6] H. Chen, L. Ran, J. Huangfu, X. Zhang, K. Chen, T. Grzegorczyk, and J. Kong, Phys. Rev. E **70**, 057605 (2004).
[7] D. Schurig, J. J. Mock, and D. R. Smith, Appl. Phys. Lett. **88**, 041109 (2006).
[8] J. D. Baena, R. Marques, F. Medina, and J. Martel, Phys. Rev. B **69**, 014402 (2004).
[9] P. Gay-Balmaz and O. J. F. Martin, Appl. Phys. Lett. **81**, 939 (2002).
[10] T. Koschny, L. Zhang, and C. M. Soukoulis, Phys. Rev. B **71**, 121103(R) (2005).
[11] J. B. Pendry, A. J. Holden, D. J. Robbins, and W. J. Stewart, J. Phys.: Condens. Matter **10**, 4785 (1998).
[12] J. B. Pendry, A. J. Holden, D. J. Robbins, and W. J. Stewart, IEEE Trans. Microwave Theory Tech. **47**, 2075 (1999).
[13] R. Marques, F. Medina, and R. Rafii-El-Idrissi, Phys. Rev. B **65**, 144440 (2002).
[14] P. A. Belov, R. Marques, S. I. Maslovski, I. S. Nefedov, M. Silveirinha, C. R. Simovski, and S. A. Tretyakov, Phys. Rev. B **67**, 113103 (2003).
[15] G. Bouchitte and D. Felbacq, SIAM J. Appl. Math. **66**, 2061 (2006).
[16] C. R. Simovski, P. A. Belov, and S. L. He, IEEE Trans. Antennas Propag. **51**, 2582 (2003).
[17] A. L. Pokrovsky and A. L. Efros, Phys. Rev. Lett. **89**, 093901 (2002).
[18] R. Marques and D. R. Smith, Phys. Rev. Lett. **92**, 059401 (2004).
[19] D. Felbacq and G. Bouchitte, Opt. Lett. **30**, 1189 (2005).
[20] S. I. Maslovski, Tech. Phys. Lett. **29**, 32 (2003).
[21] D. R. Smith, S. Schultz, P. Markos, and C. M. Soukoulis, Phys. Rev. B **65**, 195104 (2002).
[22] J. S. Derov, B. W. Turchinetz, E. E. Crisman, A. J. Drehman, S. R. Best, and R. M. Wing, IEEE Microw. Wirel. Compon. Lett. **15**, 567 (2005).
[23] V. V. Varadan, S. Puligalla, and R. Ro, Microwave Opt. Technol. Lett. **48**, 2619 (2006).
[24] D. Schurig, Int. J. Numer. Model. **19**, 215 (2006).
[25] A. I. Căbuz, Ph.D. thesis, University of Montpellier II, 2007, http://tel.archives-ouvertes.fr/tel-00161428/en/
[26] G. Russakoff, Am. J. Phys. **38**, 1188 (1970).
[27] B. Sauviac, C. R. Simovski, and S. A. Tretyakov, Electromagnetics **24**, 317 (2004).
[28] R. Marques, F. Mesa, J. Martel, and F. Medina, IEEE Trans. Antennas Propag. **51**, 2572 (2003).
[29] M. Shamonin, E. Shamonina, V. Kalinin, and L. Solymar, Microwave Opt. Technol. Lett. **44**, 133 (2005).
[30] S. Ramo, J. R. Whinnery, and T. Van Duzer, *Fields and Waves in Communication Electronics*, 3rd ed. (John Wiley and Sons, New York, 1994).
[31] I. Bahl and P. Bhartia, *Microwave Solid State Circuit Design* (John Wiley and Sons, New York, 2003).
[32] V. Yatsenko, S. Maslovski, and S. Tretyakov, Prog. Electromagn. Res. **25**, 285 (2000).
[33] V. V. Yatsenko, S. I. Maslovski, S. A. Tretyakov, S. L. Prosvirnin, and S. Zouhdi, IEEE Trans. Antennas Propag. **51**, 2 (2003).
[34] S. A. Tretyakov, F. Mariotte, C. R. Simovski, T. G. Kharina, and J. P. Heliot, IEEE Trans. Antennas Propag. **44**, 1006 (1996).
[35] J. Lekner, J. Opt. Soc. Am. A **11**, 2892 (1994).
[36] D. Felbacq, B. Guizal, and F. Zolla, Opt. Commun. **152**, 119 (1998).
[37] F. Zolla, D. Felbacq, and G. Bouchitte, Phys. Rev. E **74**, 056612 (2006).
[38] R. Petit, *Ondes Électromagnétiques en Radioélectricité et en Optique* (Masson, Paris, 1993).
[39] D. Felbacq and G. Bouchitte, Phys. Rev. Lett. **94**, 183902 (2005).
[40] D. Felbacq and G. Bouchitte, New J. Phys. **7**, 159 (2005).
[41] S. I. Maslovski, S. A. Tretyakov, and P. A. Belov, Microwave Opt. Technol. Lett. **35**, 47 (2002).
[42] A. I. Căbuz, D. Felbacq, and D. Cassagne, Phys. Rev. Lett. **98**, 037403 (2007).
[43] A. N. Grigorenko, A. K. Geim, H. F. Gleeson, Y. Zhang, A. A. Firsov, I. Y. Khrushchev, and J. Petrovic, Nature (London) **438**, 335 (2005).
[44] J. Zhou, L. Zhang, G. Tuttle, T. Koschny, and C. Soukoulis, Phys. Rev. B **73**, 041101(R) (2006).